**Water Revisited**

Frank H. Stillinger

*Science*, New Series, Vol. 209, No. 4455 (Jul. 25, 1980), 451-457.

# SCIENCE

# Water Revisited

Frank H. Stillinger

A comprehensive molecular theory for water is needed for two reasons. First, this substance is a major chemical constituent of our planet's surface and as such it may have been indispensable for the genesis of life. Second, it exhibits a fascinating array of unusual properties both in pure form and as a solvent. Physical scientists have attempted to respond

high dielectric constant; (vi) anomalously high melting, boiling, and critical temperatures for a low-molecular-weight substance that is neither ionic nor metallic; (vii) increasing liquid fluidity with increasing pressure; and (viii) high-mobility transport for $H^+$ and $OH^-$ ions.

Some of these attributes are shared with other substances; perhaps we will

*Summary.* Liquid water consists of a macroscopically connected, random network of hydrogen bonds, with frequent strained and broken bonds, that is continually undergoing topological reformation. Anomalous properties of water arise from the competition between relatively bulky ways of connecting molecules into local patterns characterized by strong bonds and nearly tetrahedral angles and more compact arrangements characterized by more strain and bond breakage. However, these alternatives constitute virtually a continuum of architectural possibilities rather than a discrete pair of options. The singular behavior of supercooled water near $-45°C$ and the "hydrophobic" attraction between nonpolar entities are due to the same underlying phenomenon, namely, the clumping tendency of relatively strain-free convex cages or polyhedra.

to this need for nearly a century, but a satisfactory molecular theory has only begun to emerge in the last decade. In this article I explain these recent developments and point out their implications for several fields.

Some of the more notable physical properties displayed by water are the following: (i) negative volume of melting; (ii) density maximum in the normal liquid range (at 4°C); (iii) isothermal compressibility minimum in the normal liquid range (at 46°C); (iv) numerous crystalline polymorphs (at least nine, including those that form at elevated pressure); (v)

eventually discover that all are. Nevertheless, it is striking that so many eccentricities should occur together in one substance.

All the properties of water and aqueous solutions ultimately must be explained in terms of the intermolecular forces that are present. Therefore, I begin with a brief look at our present understanding of water molecule interactions. This basic information then serves as input for the techniques that are now being used to predict the molecular structure and to interpret the properties of aqueous fluids. The reader may find it enlightening from a historical viewpoint to compare this survey with others on the subject by Narten and Levy (1) and by Frank (2).

## Hydrogen Bonding

The key to understanding liquid water and its solutions lies in the concept of the "hydrogen bond," which was first systematically studied by Latimer and Rodebush over half a century ago (3). In general terms it is found that specific attractions exist between electronegative atoms (such as nitrogen, oxygen, fluorine, and chlorine) and hydrogen (or deuterium) atoms, particularly when the latter are themselves chemically bonded directly to electronegative atoms (4). Hydrogen bonds are strongly directional; the chemical bond containing the hydrogen atom that is donated to the hydrogen bond tends to point directly at the nucleus of the hydrogen-accepting electronegative atom. The strengths of hydrogen bonds ($\approx 5$ kilocalories per mole) are normally intermediate between those of weak van der Waals interactions ($\approx 0.3$ kcal/mole) and those of covalent chemical bonds ($\approx 100$ kcal/mole).

The $H_2O$ molecule, which contains two hydrogen atoms and one oxygen atom in a nonlinear arrangement, is ideally suited to engage in hydrogen bonding. It can act both as a donor and as an acceptor of hydrogens. This dual ability is illustrated in vivid fashion by the crystal structure of ordinary hexagonal ice, a fragment of which is displayed in Fig. 1. Each $H_2O$ molecule in the crystal has four nearest neighbors to which it is hydrogen-bonded. It acts as hydrogen donor to two of the four and accepts hydrogens from the remaining two. These four hydrogen bonds are spatially arranged with local tetrahedral symmetry; that is, the oxygen atoms of the neighbors occupy the vertices of a regular tetrahedron surrounding the oxygen atom of the central molecule. The bond angle of the free water molecule (104.5°) is only slightly less than the ideal tetrahedral angle (109.5°) that would be required by strictly linear hydrogen bonding in the ice crystal. At 0 K the hydrogen bond lengths in the crystal (that is, the distance between neighbor oxygens) is 2.74 angstroms.

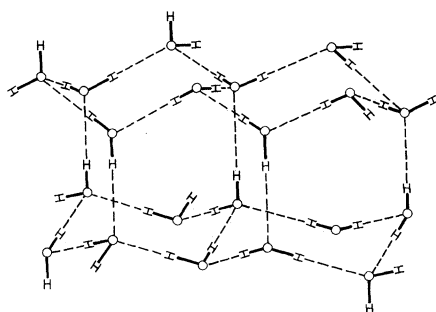If we neglect missing bonds at the crystal surface, there must be precisely two hydrogen bonds per $H_2O$ molecule

Fig. 1. Structure of hexagonal ice. Covalent chemical bonds are shown as solid lines and hydrogen bonds as dashed lines.



Fig. 2. Optimal structure of the dimer of $H_2O$, according to the molecular beam resonance studies of Dyke et al. (9).

in ice. Although a small portion of the total cohesive energy of the ice crystal is attributable to nonbonded interactions between second, third, and higher neighbors, we can nevertheless readily compute the average hydrogen bond energy from that cohesive energy to be 5.5 kcal/mole. The hydrogen bonds are sufficiently weak as compared to the chemical bonds within each of the participating water molecules that these molecules remain virtually undeformed geometrically in comparison with their free state in the dilute vapor. In particular, this implies that the hydrogen atoms sit asymmetrically along the oxygen-oxygen connecting line, with no ambiguity concerning the terminal oxygen to which each is chemically attached.

The hydrogen bonds in ice form a space-filling, three-dimensional network (Fig. 1). Starting at any oxygen atom, it is possible to traverse in many ways a closed path of contiguous hydrogen bonds by jumping always to nearest-neighbor oxygens. The smallest such polygonal paths are nonplanar hexagons. In fact, polygonal paths returning to the origin are possible with any even number of steps equal to or exceeding six. No paths of this sort comprising an odd number of steps (hydrogen bonds) exist in hexagonal ice.

The network structure of ice provides an interesting contrast to the crystal structures of the hydrides hydrogen fluoride (HF) and ammonia ($NH_3$). Although HF forms somewhat stronger hydrogen bonds than $H_2O$, these bonds form infinitely long zig-zag chains in the HF crystal (5) with no polygonal closures. With just one hydrogen atom, each HF molecule in the crystal can donate and accept hydrogens only once (unlike the double duty performed by $H_2O$ in its crystal), and so an infinite three-dimensional network of hydrogen bonds in HF is impossible. Although $NH_3$ might seem to qualify for the production of a network of hydrogen bonds, acting triply as

hydrogen donor and triply as hydrogen acceptor, the molecular size and geometry of $NH_3$ are ill suited to conform to the local arrangement of six neighbors that would be required by formation of linear hydrogen bonds of optimal length. Consequently, hydrogen bonds are severely strained and weakened in solid $NH_3$ (6). By comparison with its neighbors HF and $NH_3$ in the periodic table, $H_2O$, with the best developed network, has the highest melting point.

The propensity for $H_2O$ molecules to engage in tetrahedral hydrogen bonding extends beyond hexagonal ice to other aqueous crystals. A diverse group of clathrate hydrates has been crystallographically determined (7) and illustrates this structural theme with great clarity. Owing to the steric requirements that other molecules be included as guests in these clathrates, their hydrogen bond networks are organized somewhat differently from that of hexagonal ice. Bond lengths and angles are comparable, but the structures frequently exhibit pentagonal paths. A low-temperature cubic modification of ice is also known in which the local tetrahedral pattern of hydrogen bonds at each $H_2O$ molecule again obtains.

The directional preference for hydrogen bonding between $H_2O$ molecules tends automatically to lead to rather open network structures. If, in the hexagonal or cubic forms of ice, the $H_2O$ molecules are geometrically treated as though they were contacting rigid spheres centered at the oxygen vertices of the lattice, then the density is calculated to be only 57 percent of that for a close-packed arrangement of those spheres. The corresponding result for some of the clathrate networks can be as low as 45 percent, indicating an even more open structure.

The high-pressure ices also illustrate the tetrahedral hydrogen-bonding preference (8). For moderate pressures (ices II through VI and ice IX), some bending of hydrogen bond directions away from tetrahedral and out of linearity occurs as the system seeks higher packing densities, but an arrangement of four hydrogen-bonded neighbors remains the rule. Yet in the highest-pressure forms (ices VII and VIII) local tetrahedrality is perfectly restored as the collection of $H_2O$ molecules adopts an arrangement consisting of two interpenetrating cubic ice networks. Each $H_2O$ molecule is surrounded by eight others at equal distances, but only four of the eight are attached by hydrogen bonds.

Dimers $(H_2O)_2$ exist in the vapor phase with a structure that displays a linear hy-
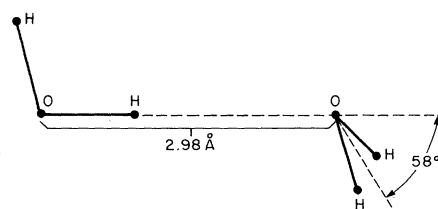
drogen bond. This structure has been revealed by molecular beam resonance experiments carried out by Dyke et al. (9) and is shown in Fig. 2. This lowest energy arrangement has a plane of symmetry containing the hydrogen donor molecule to the left and the symmetry axis of the molecule to the right. The bond length (2.98 Å) is significantly longer than the observed distance in ice, 2.74 Å.

High-accuracy quantum mechanical calculations for $(H_2O)_2$ (10) confirm the picture presented in Fig. 2, including the fact that the bond length exceeds that of ice. They also show that, starting with the most stable dimer configuration, moderate rotations of the $H_2O$ molecules about their oxygen atoms cost little energy provided the donated hydrogen remains essentially on axis. These are the rotations that are necessary to fit dimers to the network angles presented by the ice and clathrate structures. By contrast, motions that move the donated hydrogen off axis rapidly increase the dimer energy. Thus the quantum mechanical studies fully support the notion of hydrogen bond linearity, and they emphasize the opportunities for topological diversity in extended networks that stem from ease of rotation about linear hydrogen bonds.

The results of the quantum mechanical studies also are in support of an idea originally due to Frank and Wen (11) that hydrogen bonding in water is "cooperative." After forming a first hydrogen bond as in Fig. 2, the charge distribution within the participating monomers changes in such a way that the hydrogen acceptor molecule becomes potentially an even better hydrogen donor than before. In other words, it is capable of forming a stronger second bond because of the existence of the first bond. Similarly, the proton donor in Fig. 2 has an enhanced ability to accept a proton on account of the bond that it has already formed. This mutual reinforcement encourages molecules to form chains of hydrogen bonds with the mean bond energy larger and the mean bond length shorter than for the simple dimer. Although some of the bond length reduction in ice as compared to the dimer is attributable

to attractions between nonbonded molecules, the hydrogen bond cooperativity stemming from paths that thread in all directions through the crystal produces most of that reduction.

The potential energies that have been computed for $(H_2O)_2$ at a discrete set of configurations have been fitted to simple and smooth potential energy functions (10). This allows interpolation to any dimer configuration of interest. Figure 3 shows an angle bend curve for the dimer plotted for such a potential function due to Popkie *et al.* (12), based upon their extensive Hartree-Fock self-consistent field computations. This graph illustrates the important qualitative point that the characteristic tetrahedral orientation angles ($\theta = \pm 54.7°$ in this representation) do not appear as prominent separate minima. This fact contradicts suggestions (13) that these angles are preferred in nature because they align lone-pair electrons (in suitably hybridized $sp^3$ molecular orbitals) along the hydrogen-bond axis. Nor do quantum mechanical studies of hydrogen bond cooperativity cause any essential change in this fact. The preeminence of tetrahedral coordination instead arises as the only feasible way to arrange mutually repelling neighbors around a central water molecule at distances close enough to permit fully developed hydrogen bonds. Any attempt to incorporate a fifth neighbor leads to severe crowding and possible loss of already-formed hydrogen bonds. Such high-energy configurations would not be expected to occur frequently in liquid or solid phases at ordinary pressures.

## Pure Liquid Water

The melting of ice to produce liquid water obviously entails basic changes in the way that the molecules are arranged relative to one another. Rigidity is replaced by fluidity, and crystalline periodicity gives way to spatial homogeneity. Molecules are much freer to diffuse about and to change their orientation, and melting has caused the density to increase by about 9 percent. Any acceptable molecular theory for liquid water must account for the topology and geometry of the hydrogen bond network after it has been altered by the melting process.

Although no single experiment or combination of experiments is capable of characterizing the molecular architecture of the liquid network in detail, some key measurements provide important guidelines concerning how the detailed description can be phrased. For
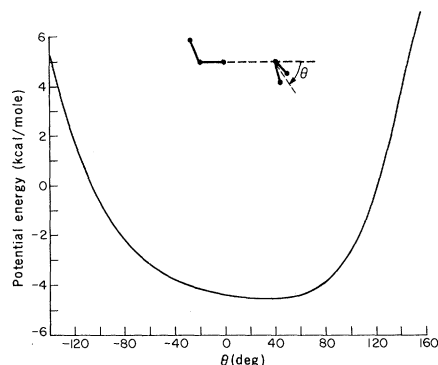
Fig. 3. Dimer potential energy plotted as a function of the hydrogen acceptor bend. This curve utilizes the fit function constructed by Popkie *et al.* (12) to represent their Hartree-Fock self-consistent field (molecular orbital) calculations. The oxygen-oxygen distance is 3.00 Å.

example, the heat of melting is only 13 percent of the sublimation energy of the solid; this result may be interpreted to mean that a comparable percentage of hydrogen bonds rupture upon melting. Even though the actual rupture percentage may be somewhat higher since more favorable alignment of nonnearest neighbors can occur in the liquid than in the solid, it seems safe to conclude that the majority of hydrogen bonds survive the trauma of melting.

Diffraction of x-rays (14) and of neutrons (15) by water provides further important information. The x-ray diffraction patterns are sensitive primarily to the distribution of distances between pairs of oxygen atoms in the liquid. The neutron diffraction patterns (especially if isotopically substituted water is used) add the corresponding distance distributions for pairs of hydrogens and for mixed oxygen-hydrogen pairs. These complementary techniques reveal that the mean separation between nearest neighbors in ice increases by 0.1 Å upon melting, and the number of nearest neighbors increases to 4.5 to 5.0 (depending on what maximum distance is selected for counting "nearest" neighbors). A broad second neighbor distribution is found in the oxygen-oxygen distance range where successive bonds at the tetrahedral angle would require them to occur. The combined diffraction evidence is strongly in support of the persistence of tetrahedral hydrogen-bond order beyond the melting transition, but with substantial disorder present.

Important questions remain about the precise nature of that disorder and how it is spatially manifest. The available measurements on liquid water simply do not lead uniquely to a clear picture. Fortunately, there is another source

for the missing information, the technique of "computer simulation." Provided one has a reliable way to calculate intermolecular potentials, the simulations are devised so as to generate a representative set of configurations for a small region within the solid or liquid of interest, containing typically $10^2$ to $10^3$ molecules. These configurations, or "snapshots," of the molecular medium may either be disconnected in time [from the "Monte Carlo" simulation method (16)] or they may be chronologically ordered so as to provide a submicroscopic movie of the dynamical motions [from the molecular dynamics simulation method (17)]. In either case, the investigator has control over the thermodynamic parameters of state such as temperature and density, and from the computer output he is able to observe preferred molecular arrangements and to calculate static and (for the molecular dynamics method) kinetic properties. Both variants of the simulation technique have been applied to liquid water.

Since hydrogen bonding is the most important interaction in liquid water and since these interactions are cooperative (that is, nonadditive), it is insufficient for the purposes of computer simulation to use the potential energy function for dimers alone. Those using computer simulation thus have been compelled to include in their programs either explicit many-molecule potentials or "effective" pair potentials which incorporate the increased binding effect of cooperativity (18).

Although the computer simulation studies of water and aqueous solutions have some characteristic weak points (small system size, short time spans, difficulty of including quantum corrections), it has been gratifying to see many of the key attributes of water automatically emerge, for example, the liquid-phase density maximum phenomenon, isothermal compressibility minimum, and high heat capacity. Furthermore, the rates of translational and rotational diffusion observed in the molecular dynamics simulations stand in moderately good agreement with experiment. Finally, the x-ray and neutron diffraction patterns inferred from the simulations have the correct general appearance for liquid water (17). Although there is still room for quantitative improvement, one can be satisfied that a qualitatively "water-like" substance has indeed been created by digital computer.

With these successes at mimicking available experiments as background, one is encouraged to look more deeply into the computer simulations to find an-
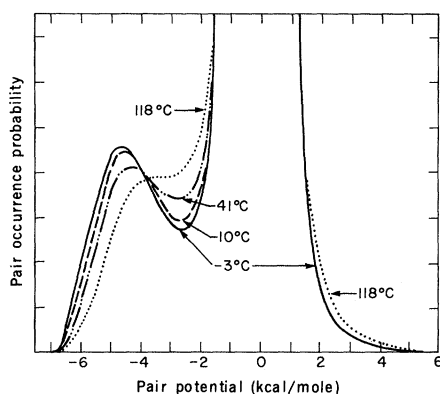
Fig. 4. Distribution function for effective pair interactions between molecules in liquid water (at 1 gram per cubic centimeter). [Redrawn from (17)]
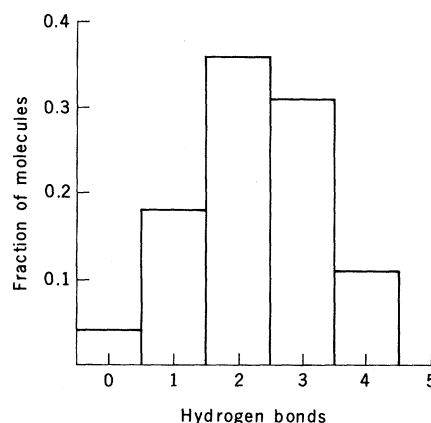


Fig. 5. Fractions of molecules in liquid water engaging in various numbers of hydrogen bonds. These results refer to the liquid at 10°C and with a density of 1 g/cm³ (17).

swers that are not accessible by experiment. In particular, the simulations are well suited for identifying the types of hydrogen-bond geometric patterns that are present in liquid water.

Even though there is hardly any uncertainty about what constitutes a pair of hydrogen-bonded molecules in ice, the more diverse set of local arrangements in the liquid can lead to ambiguity on this point. Obviously a precise criterion for the existence of a hydrogen bond has to be formulated if a computer is to be instructed to identify bonds in molecular configurations generated by a simulation study. The most direct criterion uses the potential energy of interaction itself and defines the hydrogen bond to exist between two molecules whenever their (effective) pair potential drops below some negative critical value $V_{HB}$. By choosing a specific $V_{HB}$ in the neighborhood of $-4$ kcal/mole, one has a criterion which automatically agrees with the intuitive understanding of the structure of ice (four bonds to nearest neighbors, and none to further neighbors) and which is applicable with precision to the liquid.

At first glance, the introduction of the critical potential $V_{HB}$ for hydrogen bonding may seem arbitrary. Yet the behavior of liquid water as revealed by the simulations strongly suggests a natural choice for $V_{HB}$. Figure 4 shows how the effective molecular pair interactions $V^{(2)}$ are distributed in the liquid at four temperatures, according to a molecular dynamics simulation (17). The strong divergence around $V^{(2)} = 0$ is uninteresting; it simply reflects the large number of widely separated and therefore weakly interacting pairs. Bonded neighbors show up at negative $V^{(2)}$. A few repelling pairs appear at large positive $V^{(2)}$. The significance of Fig. 4 lies in the point at $-4.0$ kcal/mole, which is virtually in-

variant to temperature changes. It appears that a thermally activated bond breakage is at work which transfers pairs across this invariant point as temperature rises. Choosing $V_{HB}$ to be the value of $V^{(2)}$ at the invariant point then is natural both for the solid and for the liquid.

Having thus formulated a precise working definition of the hydrogen bond, one can begin to probe the statistical geometry and topology of the hydrogen bond network. An obvious question is what fractions of the molecules at any instant are connected, respectively, by 0, 1, 2, . . . hydrogen bonds. Figure 5 shows a typical result, in this instance referring to water at 10°C (17). The histogram represents a relatively broad distribution about a mean number of 2.3 hydrogen bonds to each molecule. At different temperatures the corresponding histograms look similar, but, as expected, the mean of the distribution shifts with rising temperature to lower numbers of hydrogen bonds.

Although the distribution in Fig. 5 may seem unremarkable, it nevertheless appears to rule out a large class of models for liquid water, the "framework-interstitial" models. In these models it is postulated that some totally unbonded water molecules reside at interstitial sites within a fully bonded host framework. The latter has variously been described as a clathrate structure (19) and as a slightly deformed hexagonal ice structure (1). In any case these models require a bimodal distribution in a plot of the type shown in Fig. 5, with maxima at no hydrogen bonds and at four hydrogen bonds. No computer simulation study has ever spontaneously produced such a result. The small fractions found in the simulations for water with no hydrogen bonds agree with conclusions that have been formulated on spectroscopic grounds (20).

By applying a suitable pattern-search routine to molecular configurations for liquid water that have been produced in simulations, one is able to observe the way in which hydrogen bonds tend to be organized into polygons (21). Figure 6 shows the relative concentrations of hydrogen bond polygons for the same thermodynamic state to which Fig. 5 referred, 10°C. These are non–short-circuited polygons, that is, those with no cross-connections which would break them into a pair of smaller polygons. In this way of reckoning, hexagonal ice would consist entirely of hexagons (all its other even polygons are short-circuited). Both even and odd polygons are present (Fig. 6), with no notable prefer-

ence for one over the other. It is immediately obvious then that liquid water cannot be topologically related to hexagonal (or cubic) ice by mere bond scission, whether random or not. This last observation rules out "iceberg" models of water that postulate disconnected fragments of ice suspended in a sea of unbonded water molecules (22).

The number of hydrogen bonds, their multiplicities of incidence at single molecules, and their organization into non-short-circuited polygons are all local properties of the aqueous fluid. A global characteristic is the extent of macroscopic connectivity of the collection of hydrogen bonds. At least for water around room temperature and below, it has been demonstrated by computer simulation (23) that the liquid lies above the "critical percolation threshold" for hydrogen bonding; that is, any macroscopic sample of the liquid inevitably will have uninterrupted hydrogen bond paths running in all directions, spanning the entire volume of the sample. The liquid in the large is communally connected. These network pathways, incidentally, provide natural routes for rapid transport of $H^+$ and $OH^-$ (a proton "hole") by a directed sequence of exchange hops (4). Although rare unconnected clusters of one, two, three, . . . molecules can in principle appear within the medium, any suggestion that disconnected "icebergs" of any internal structure ought to dominate the description receives no support.

The view of liquid water that does emerge collectively from these results is that of a random, three-dimensional network of hydrogen bonds. This network has a local preference for tetrahedral geometry, but it contains a large proportion of strained and broken bonds. These strained bonds appear to play a funda-

mental role in kinetic properties, because their presence enhances prospects for molecules to switch allegiances, trading a bond here for one there and thus altering the network topology. This general description has been supported and enriched with extra detail as a result of an examination of stereoscopic picture pairs for selected molecular configurations (24).

The melting of ice permits the water molecules to occupy less space by utilizing relatively compact network patterns (polygons and polyhedra) with substantial hydrogen bond strain. Of course, there is an energy penalty for this conversion paid as the latent heat of melting. The conversion to more packing-efficient and more strained patterns continues as the liquid is heated to 4°C. But a competitive process is present as well, the rupture of hydrogen bonds, which tends to cause overall expansion since nonbonded neighbors normally reside farther from one another than those that are bonded. Above 4°C, the effects of this latter process dominate to produce a normal positive coefficient of thermal expansion.

## Supercooling

The careful study of the properties of supercooled water, principally by Angell and his collaborators, provides a fascinating addendum to the already interesting catalog of aqueous properties (25). The interpretation of these results yields new insights into the nature of the random hydrogen bond network. The principal observation is that virtually all properties measured appear headed for an anomaly at $T_s \approx -45°C$, just below the limit of attainable supercooling at about $-41°C$. The constant-pressure heat capacity $C_p$ is a case in point, since it has risen at this limit to nearly 30 calories per mole per degree Celsius from the value of 18 cal mole$^{-1}$ deg$^{-1}$ at the normal freezing point. Furthermore, the $C_p$ data can best be fitted to a fractional-power-law form that actually diverges to infinity at $T_s$, and which therefore closely resembles diverging heat capacities that are encountered at critical points for liquid-vapor transitions, binary alloy order-disorder transitions, and magnetic transitions (26). The strong implication is that some kind of structural order-disorder phenomenon must be at work in the hydrogen bond network of supercooled water to produce the observed anomalies.

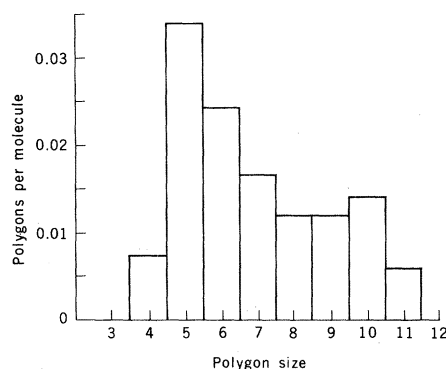Although it is possible in principle to investigate the molecular structure of su-

Fig. 6. Concentrations of non–short-circuited hydrogen bond polygons in water at 10°C. [Adapted from (21)]

percooled water by computer simulation, a practical difficulty stems from the fact that all relaxation processes slow down drastically as the temperature declines into the deep supercooling regime. Consequently, it becomes increasingly difficult to compute a representative set of network configurations for the metastable state starting, as one must, from a higher temperature state. Unfortunately, the greatest difficulty occurs in the most interesting temperature range, that approaching $T_s$. Nevertheless, enough has been learned about water networks at and above 0°C so that by extrapolation it is possible to put together a credible qualitative account that explains the supercooling behavior.

The important issue for supercooling appears to be the concentration and spatial distribution of relatively unstrained (and hence bulky) hydrogen bond polyhedra embedded within and linked to the random network. Figure 7 shows in schematic fashion a few of these out of the many possibilities, including an octameric unit (Fig. 7a) that occurs throughout hexagonal ice. At least above the

equilibrium freezing point these unstrained polyhedra would be infrequent occurrences in the largely strained and defective network but not absent altogether.

Model building reveals that the hydrogen bond angles naturally present in many of these polyhedra make it easy for them to share edges and faces without the introduction of mutual strain. Consequently, they are able to link up with one another more readily than a strained and an unstrained polyhedron can, on the average. As a result, the ideal unstrained structures find it advantageous to clump together; they experience a mean attraction for one another.

The situation just described is one in which a condensation phenomenon can arise. At temperatures close to 0°C, the infrequent unstrained polyhedra form a dilute "gas" dispersed throughout the predominantly strained and defective network. But as temperature declines, the polyhedra become more and more frequent since they incorporate stronger hydrogen bonds. As their concentration rises, they will aggregate under the influence of the cited mean attraction to form larger and larger clumps or clusters. By analogy with the vapor-liquid condensation process, the last stage of polyhedron aggregation would be expected to produce cluster sizes that diverge as $T_s$ is approached from above.

Two obvious macroscopic properties reveal the presence of the aggregation process. First, the density declines with decreasing temperature at a rate diverging at $T_s$ (5), showing that the overall concentration of low-density structural elements is increasing dramatically. Second, the shear viscosity exhibits a divergence at $T_s$ (5), just as would be expected for a medium containing relatively rigid regions, the well-bonded aggre-
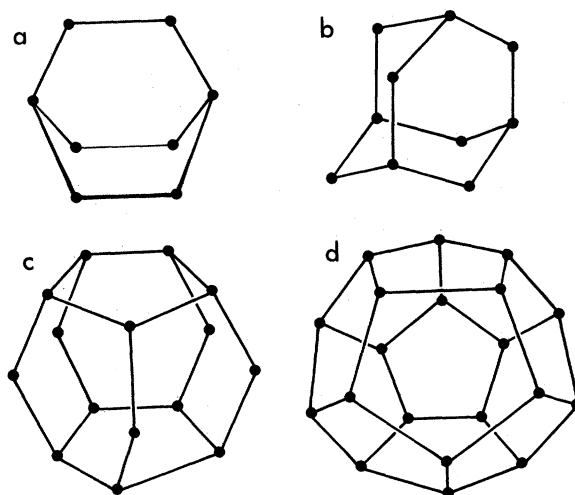
Fig. 7. Bulky, unstrained polyhedra formed by hydrogen-bonded water molecules (not explicitly shown). Positions of oxygen nuclei are shown as circles, and bond angles at these vertices are close to tetrahedral. External bonds to the surrounding network are not shown.

gates, of diverging average size (27).

Just as density fluctuations produce large light scattering at the liquid-vapor critical point (26), the low-density well-bonded aggregates near $T_s$ should also produce anomalous light scattering. The related light-scattering experiments unfortunately have not yet been done.

A more detailed form of the argument just outlined explains each of the thermodynamic anomalies of supercooled water (27).

## Hydrophobic Interactions

The behavior of water toward nonpolar solutes (and nonpolar side groups attached to biopolymers) has long been recognized as unusual. This peculiarity and its effects have given rise to the popular phrases "hydrophobic effect" and "hydrophobic bond," which remain in fashion in spite of Hildebrand's semantic objections (28). Details are available in a review by Franks (29) and a recent book by Ben-Naim (30).

Typical nonpolar solutes are the noble gases, hydrocarbons such as methane and cyclopropane, and sulfur hexafluoride. None can readily hydrogen bond to water, and all are sparingly soluble. The process of isothermally dissolving such substances in water is accompanied by a significant negative entropy that quite naturally has been interpreted as a "structure-making" phenomenon in that solvent. Any acceptable molecular theory must account for this "hydrophobic interaction."

Nonpolar solutes occupy space. If a nonpolar solute molecule is to be placed in liquid water, the random hydrogen bond network must reorganize around it in such a way that sufficient room is available to accommodate that molecule while at the same time not causing (if possible) too much extra damage to the already defective hydrogen bond network. The crystal structures of the clathrate hydrates for many of these nonpolar substances show that such rearrangements are possible in principle.

Once again, computer simulation offers the best opportunity to understand details of the solvation process at the molecular level. Several studies of this sort (31) seem to agree that insertion of a single space-filling but otherwise essentially inert solute molecule spontaneously causes the network to rearrange toward formation of a local clathrate-like convex cage. As might be expected, however, the cage is usually far from perfect. Although there is some strengthening of hydrogen bonds in the cage rela-
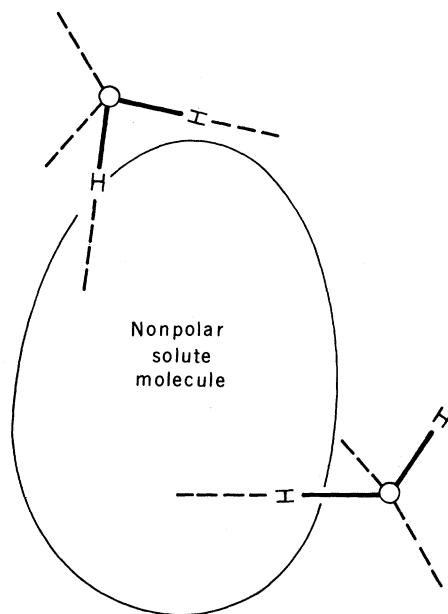


Fig. 8. Orientational preference for water molecules next to a nonpolar solute. In order to preserve intact the maximum number of hydrogen bonds, the water molecules tend to straddle the inert solute, pointing two or three tetrahedral directions tangential to the surface of the occupied space.

tive to the case in pure water, substantial strain and disorder remain. Evidently the surrounding medium with its own strained and broken bonds exerts strong forces and torques on the solvent sheath, which cause geometric disruption.

The negative entropy for the solution of nonpolar molecules resides partly in the strengthening of the bonds in the imperfect solvation cage. But it is also related to the fact that molecules in that cage layer around the solute have markedly reduced orientational options. Because of the energetic advantage of having hydrogen bonds rather than of not having them, each solvation sheath water molecule strongly prefers to place its tetrahedral bonding directions (OH covalent bonds, and the "lone pair" directions) in a straddling mode (Fig. 8). This arrangement obviously permits bonding to other solvation layer water molecules and always avoids pointing one of the four tetrahedral directions inward toward the region occupied by the inert solute, which would "waste" a possible hydrogen bond. Computer simulation unequivocally supports these orientational preferences.

Pairs of nonpolar solutes in water experience an entropy-driven net attraction for one another, the so-called "hydrophobic bond." These hydrophobic pair interactions are generally thought to be an important determinant for the native conformation of biopolymers containing both hydrophobic and hydrophilic side

groups (32). The accepted qualitative explanation for the attraction is that, when two nonpolar molecules are close together, their joint solvation cage entails less overall order and hence less entropy reduction than when those solutes are far apart. There is, in other words, a thermodynamically driven tendency toward the sharing of orientationally inhibited solvation sheath molecules.

We can now see that a logical relation exists between hydrophobic pair interactions and supercooled water anomalies. Insertion of a nonpolar solute molecule into water biases the configurational probabilities for water molecules in its immediate vicinity toward formation of a convex hydrogen bond polyhedron of sufficient size to contain that solute. Although the geometry of the solvation cage is usually not a perfect clathrate-type cage, the solute still can be regarded as a marker for a location in the water at which ideal convex polyhedra are most likely to occur. The mean attraction of such biased regions is just the mean attraction cited above as underlying the anomalous behavior of supercooled water. The well-documented apparent attraction of nonpolar entities for one another in water is thus merely another facet of the clumping tendency for well-formed (but empty) convex structures in pure supercooled water. In computer simulation studies a preference has been observed for pairs of solute particles to inhabit edge or face-sharing convex cages (31).

Volumetric experiments carried out on homologous series of alcohols (33) suggest that nonpolar solutes in water would raise the temperature of maximum density. Such an influence, if correct, no doubt would have to be due to the enhanced concentration of bulky cage structures. (Ionic solutes are known to have the contrary effect since their strong electric fields twist water molecules out of orientations that can bond easily to the surrounding network.) The foregoing discussion then leads one to suspect that the addition of nonpolar solutes to supercooled water should also cause a rise in the "critical temperature" $T_s$. The relevant experiments have not yet been undertaken but clearly deserve serious consideration.

### References and Notes

1. A. H. Narten and H. A. Levy, *Science* **165**, 447 (1969).
2. H. S. Frank, *ibid.* **169**, 635 (1970).
3. W. M. Latimer and W. H. Rodebush, *J. Am. Chem. Soc.* **42**, 1419 (1920).
4. Several detailed treatises on hydrogen bonding are available. Recent examples are those by S. N. Vinogradov and R. H. Linnell [*Hydrogen Bonding* (Van Nostrand Reinhold, New York, 1971)] and P. Schuster, G. Zundel, C. Sand-

orfy, Eds. [*The Hydrogen Bond*, vol. 1, *Theory*; vol. 2, *Structure and Spectroscopy*; vol. 3, *Dynamics, Thermodynamics, and Special Systems* (North-Holland, Amsterdam, 1976)].
5. M. Atoji and W. N. Lipscomb, *Acta Crystallogr.* **7**, 173 (1954).
6. I. Olovsson and D. H. Templeton, *ibid.* **12**, 832 (1959).
7. D. W. Davidson, in *Water, A Comprehensive Treatise*, F. Franks, Ed. (Plenum, New York, 1973), vol. 2, p. 115.
8. D. Eisenberg and W. Kauzmann, *The Structure and Properties of Water* (Oxford Univ. Press, New York, 1969), chap. 3.
9. T. R. Dyke, K. M. Mack, J. S. Muenter, *J. Chem. Phys.* **66**, 498 (1977).
10. The calculations are reviewed in F. H. Stillinger, *Adv. Chem. Phys.* **31**, 1 (1975); see also P. Schuster, in *The Hydrogen Bond*, P. Schuster, G. Zundel, C. Sandorfy, Eds. (North-Holland, Amsterdam, 1976), vol. 1, p. 25.
11. H. S. Frank and W. Y. Wen, *Discuss. Faraday Soc.* **24**, 133 (1957); H. S. Frank, *Proc. R. Soc. London Ser. A* **247**, 481 (1958).
12. H. Popkie, H. Kistenmacher, E. Clementi, *J. Chem. Phys.* **59**, 1325 (1973).

13. N. Bjerrum, *Science* **115**, 385 (1952); L. Pauling, *The Nature of the Chemical Bond* (Cornell Univ. Press, Ithaca, N.Y., ed. 3, 1960).
14. A. H. Narten and H. A. Levy, *J. Chem. Phys.* **55**, 2263 (1971).
15. A. H. Narten, *ibid.* **56**, 5681 (1972).
16. S. Swaminathan and D. L. Beveridge, *J. Am. Chem. Soc.* **99**, 8392 (1977).
17. F. H. Stillinger and A. Rahman, *J. Chem. Phys.* **60**, 1545 (1974).
18. F. H. Stillinger, *J. Phys. Chem.* **74**, 3677 (1970).
19. L. Pauling, in *Hydrogen Bonding*, D. Hadzi and H. W. Thompson, Eds. (Pergamon, London, 1959), p. 1.
20. D. P. Stevenson, *J. Phys. Chem.* **69**, 2145 (1965).
21. A Rahman and F. H. Stillinger, *J. Am. Chem. Soc.* **95**, 7943 (1973).
22. G. Nemethy and H. A. Scheraga, *J. Chem. Phys.* **36**, 3382 (1962).
23. A. Geiger, F. H. Stillinger, A. Rahman, *ibid.* **70**, 4185 (1979).
24. A. Rahman and F. H. Stillinger, *ibid.* **55**, 3336 (1971); W. L. Jorgensen, *Chem. Phys. Lett.*, in press.
25. C. A. Angell, in *Water, A Comprehensive Treat-*

*ise*, F. Franks, Ed. (Plenum, New York, in press), vol. 7.
26. H. E. Stanley, *Introduction to Phase Transitions and Critical Phenomena* (Oxford Univ. Press, New York, 1971).
27. F. H. Stillinger, in *Water in Polymers*, S. P. Rowland, Ed. (American Chemical Society, Washington, D.C., in press).
28. J. H. Hildebrand, *J. Phys. Chem.* **72**, 1841 (1968).
29. F. Franks, in *Water, A Comprehensive Treatise*, F. Franks, Ed. (Plenun, New York, 1975), vol. 4, p. 1.
30. A. Ben-Naim, *Hydrophobic Interactions* (Plenum, New York, 1980).
31. V. G. Dashevsky and G. N. Sarkisov, *Mol. Phys.* **27**, 1271 (1974); J. C. Owicki and H. A. Sheraga, *J. Am. Chem. Soc.* **99**, 7413 (1977); S. Swaminathan, S. W. Harrison, D. L. Beveridge, *ibid.* **100**, 5705 (1978); A. Geiger, A. Rahman, F. H. Stillinger, *J. Chem. Phys.* **70**, 263 (1979); C. Pangali, M. Rao, B. J. Berne, *ibid.* **71**, 2982 (1979).
32. W. Kauzmann, *Adv. Protein Chem.* **14**, 1 (1959).
33. G. Wada and S. Umeda, *Bull. Chem. Soc. Jpn.* **35**, 646 (1962).

# The Phylogeny of Prokaryotes

G. E. Fox, E. Stackebrandt, R. B. Hespell, J. Gibson

J. Maniloff, T. A. Dyer, R. S. Wolfe, W. E. Balch

R. S. Tanner, L. J. Magrum, L. B. Zablen, R. Blakemore

R. Gupta, L. Bonen, B. J. Lewis, D. A. Stahl

K. R. Luehrsen, K. N. Chen, C. R. Woese*

A revolution is occurring in bacterial taxonomy. What had been a dry, esoteric, and uncertain discipline—where the accepted relationships were no more than officially sanctioned speculation—is becoming a field fresh with the excitement of the experimental harvest. For the most part the transition reflects the realization that molecular sequencing techniques permit a direct measurement of genealogical relationships.

Bacterial genealogies appear to be far more ancient than their eukaryotic counterparts. For this reason techniques that have worked so well in establishing eukaryotic phylogenies—such as comparative analysis of cytochrome c sequences (*1*)—are of limited value when applied to the bacteria. However, by the choice of the properly constrained molecule, the molecular approaches to phylogeny that have proved to be successful for eukaryotes can readily be extended to the bacterial domain. The molecules of choice in this instance appear to be the ribosomal RNA's

(rRNA's). They are universally distributed, exhibit constancy of function, and appear to change in sequence very slowly—far more slowly than most proteins. Moreover, they are readily isolated.

Over the past decade, comparative analysis of the 16S ribosomal RNA sequence has been used to explore prokaryote phylogeny. For the most part these studies have been carried out at the University of Illinois. However, the cyanobacterial characterizations discussed below have been done at Dalhousie. To date more than 170 individual species have been characterized in this way (*2–*

*16*). In this article we summarize these results and provide a first glimpse of the outline of prokaryotic phylogeny.

Experimental details of the approach and the methods of data analysis have been described (*3, 4, 17*). In summary: $^{32}$P-labeled 16S rRNA from a given species is digested with ribonuclease T1, and the resulting oligonucleotides are resolved by two-dimensional paper electrophoresis (*17*) and then sequenced—thus producing a catalog of sequences characteristic of the organism. Comparisons of these catalogs—which is tantamount to comparing the original 16S rRNA sequences—reveals the genealogical relationships among the organisms considered. These relationships can be quantified in terms of an association coefficient, $S_{AB}$, which is calculated for each binary pair. Dendrograms are then obtained by cluster analysis (average linkage between the merged groups) (*18*). Unfortunately, this association coefficient is related to the actual number of nucleotide differences between the underlying 16S rRNA sequences in an unknown and nonlinear way. Hence the usual methods of tree construction (that is, the matrix method) have not been employed, since it is unclear how the branch lengths should be interpreted. Nevertheless the analysis appears to yield a good approximation to the true phylogenetic relationships provided that